Supplementary Information

Radical–quinone chain suppression in Catechyl lignin via isocyanate modification for permanently whitened and dispersible optical additives

Chenli Wu[a,b,c], Dexin Chen[e], Qinyu Wang[b,c], Qiang Liu[b,d], Shihao Su[b,c]*, Lei Wang[b,c,d]*

[a]College of Environmental and Resource Sciences, Zhejiang University, Hangzhou 310058, Zhejiang Province, China

[b]Zhejiang Key Laboratory of Low-Carbon Intelligent Synthetic Biology, School of Engineering, Westlake University, Hangzhou, Zhejiang 310030, China

[c]Institute of Advanced Technology, Westlake Institute for Advanced Study, Hangzhou, Zhejiang 310024, China

[d]Center for Biobased Materials, Muyuan Laboratory, 110 Shangding Road, Zhengzhou 450016, Henan Province, China

[e]Center of Artificial Photosynthesis for Solar Fuels and Department of Chemistry, School of Science and Research Center for Industries of the Future, Westlake University, Hangzhou 310030, Zhejiang Province, China

*Corresponding authors: sushihao@westlake.edu.cn; wang_lei@westlake.edu.cn

1. Figures and tables

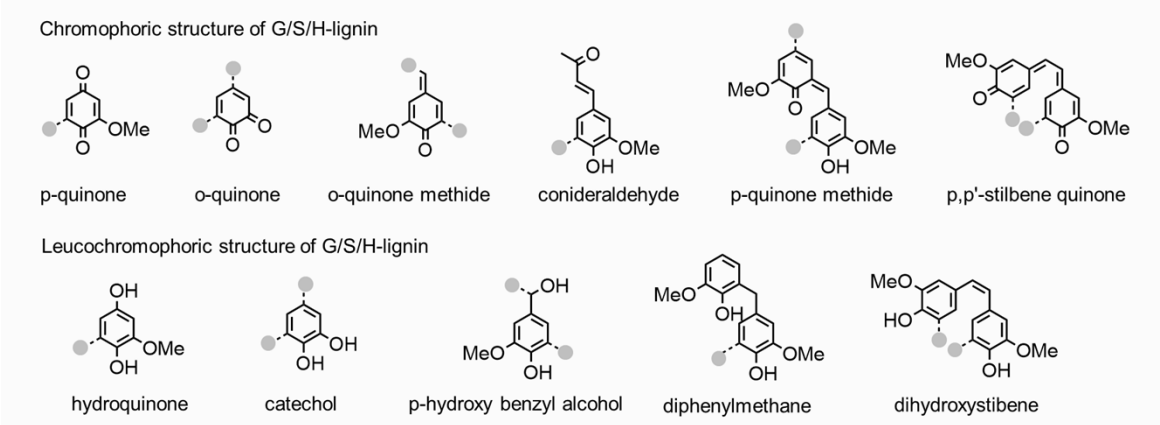

Figure S1. Major intrinsic chromophores in lignin are responsible for its native coloration.

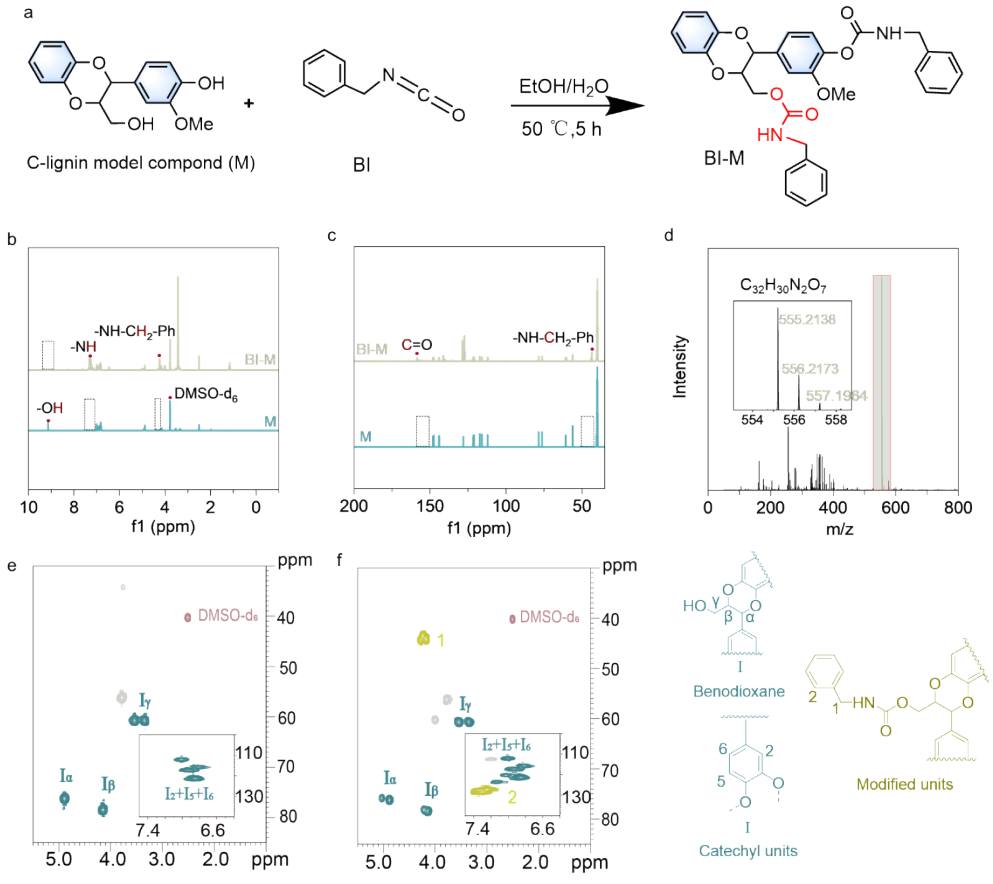

Figure S2. Structural confirmation of BI–M formation. a)scheme of reaction, b)^{1}H NMR spectra, c) ^{13}C NMR of M and BI–M in DMSO-d_6, d) HRMS (ESI^{+}) of BI–M showing the diagnostic $[M+H]^{+}$ ion at m/z 555.2138 with the expected isotopic pattern. e-f) 2D HSQC spectra of M and BI–M

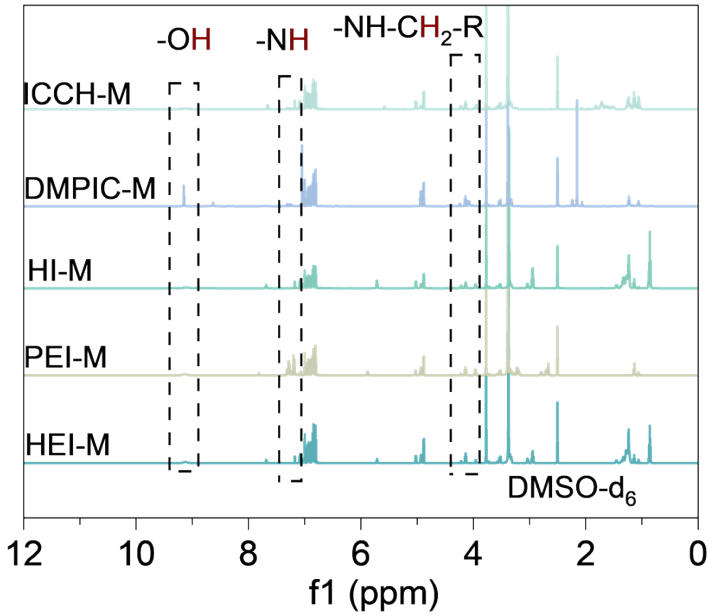

32

33 **Figure S3.** ^{1}H NMR of M modified by HEI, PEI, HI, 2,6-DMPIC, and ICCH

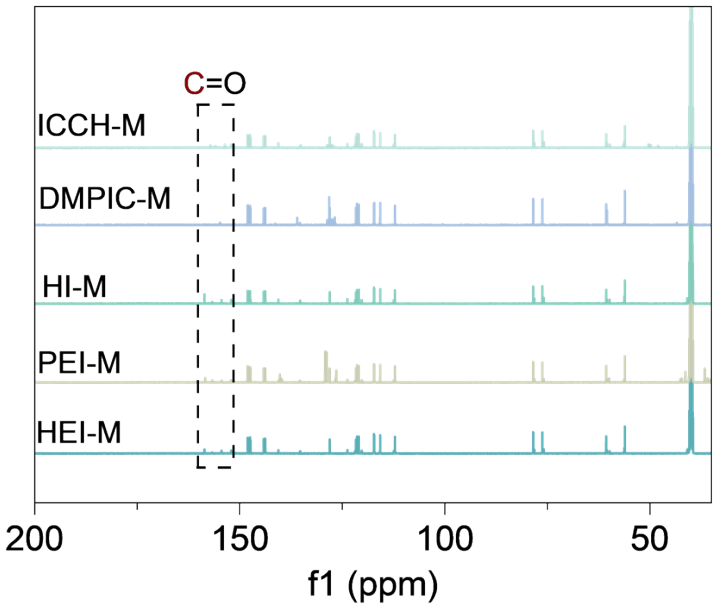

34

35 **Figure S4.** ^{13}C NMR NMR spectrum of M by HEI, PEI, HI, 2,6-DMPIC, and ICCH

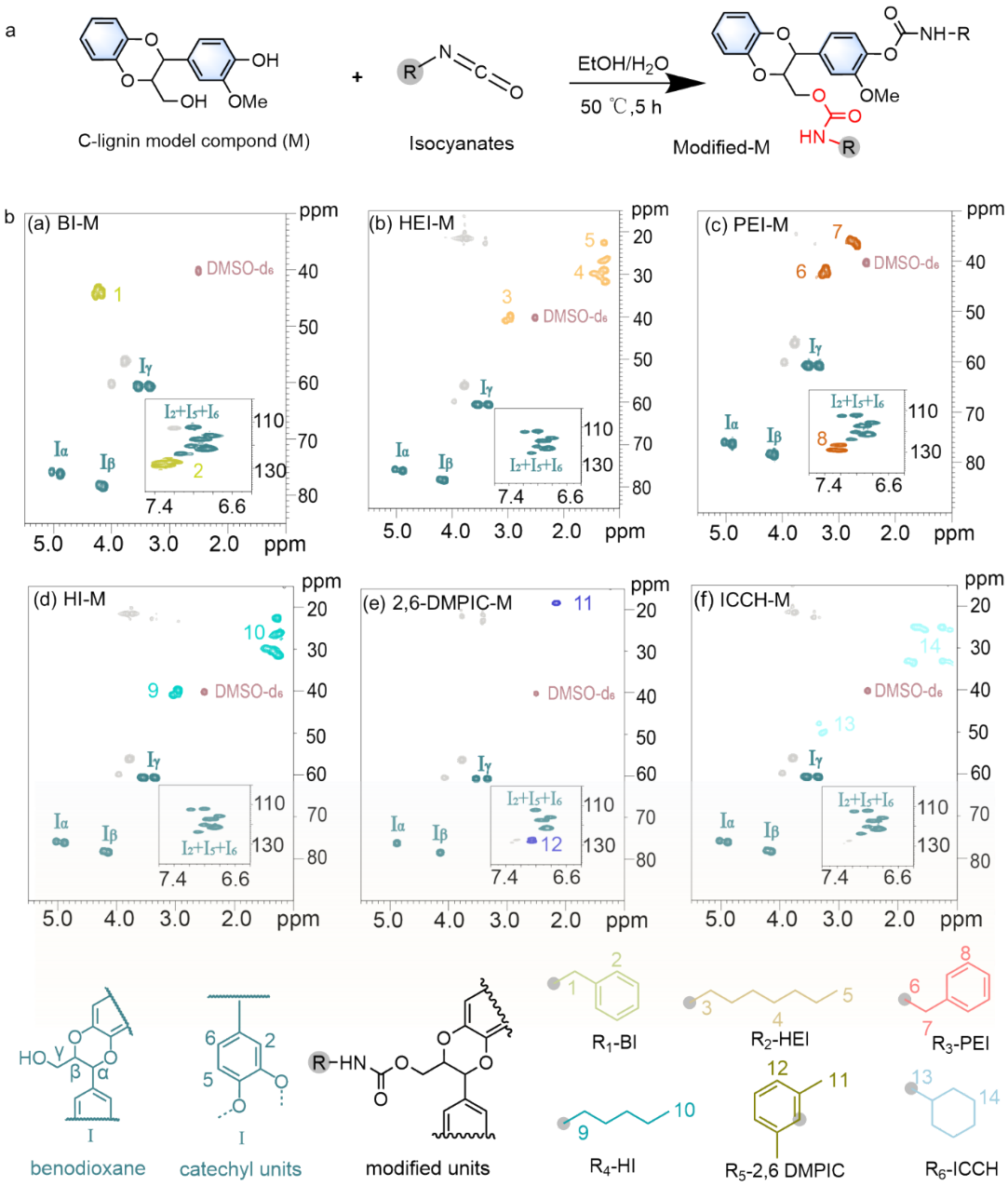

Figure S5. 2D HSQC NMR spectrum of M modified by (a) BI, (b) HEI, (c) PEI, (d) HI, (e) 2,6-DMPIC, and (f) ICCH

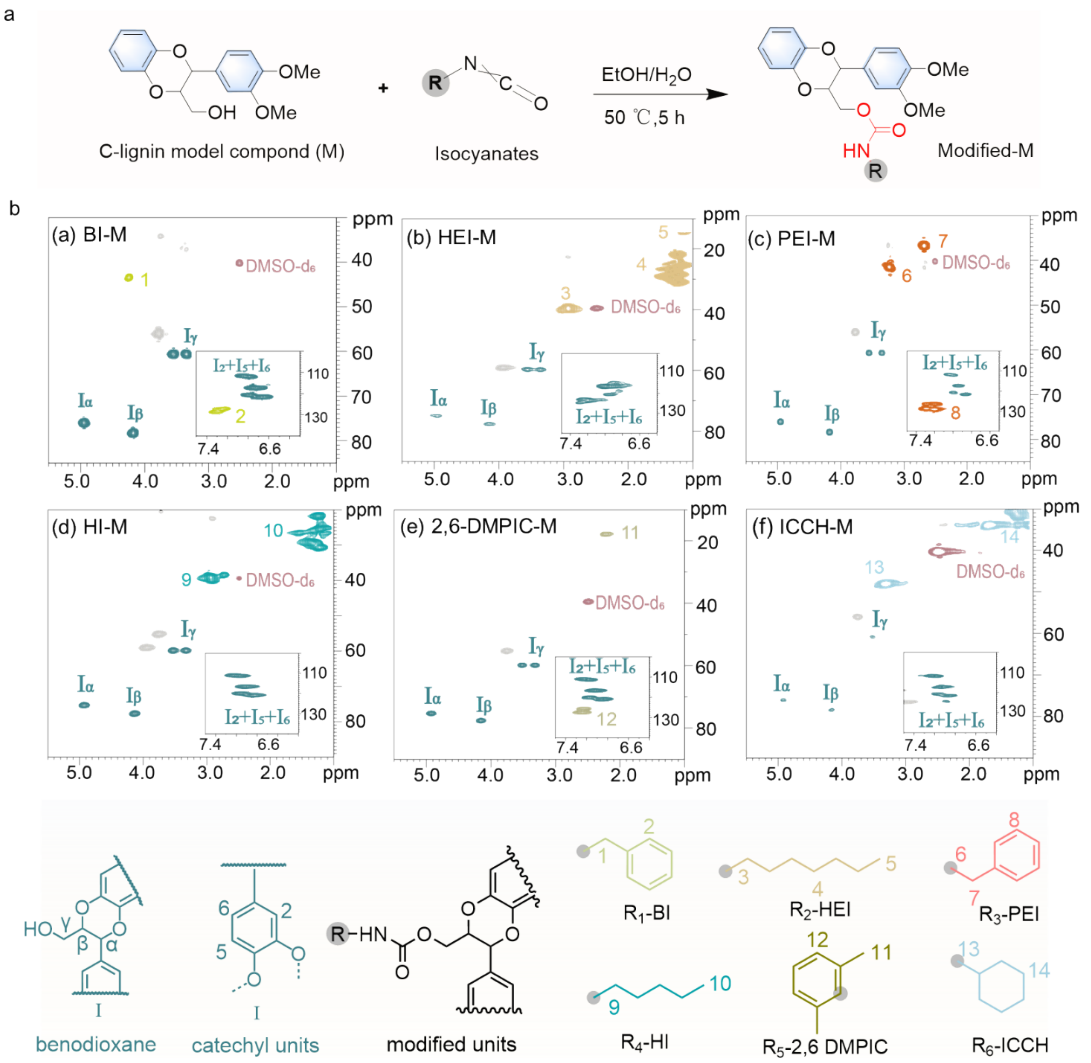

Figure S6. 2D HSQC NMR spectrum of M' modified by (a) BI, (b) HEI, (c) PEI, (d) HI, (e) 2,6-DMPIC, and (f) ICCH

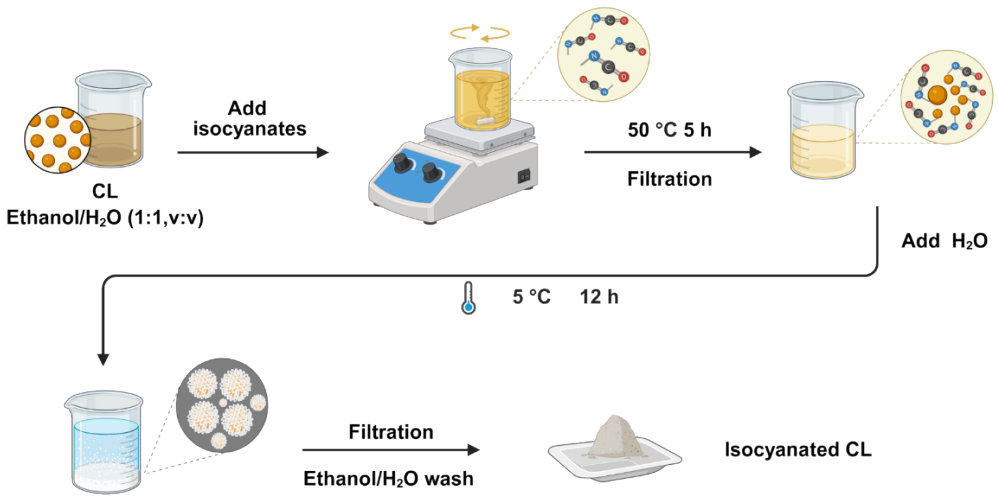

Fi

46 **gure S7.** The process flowchart of CL modified by isocyanates.

47

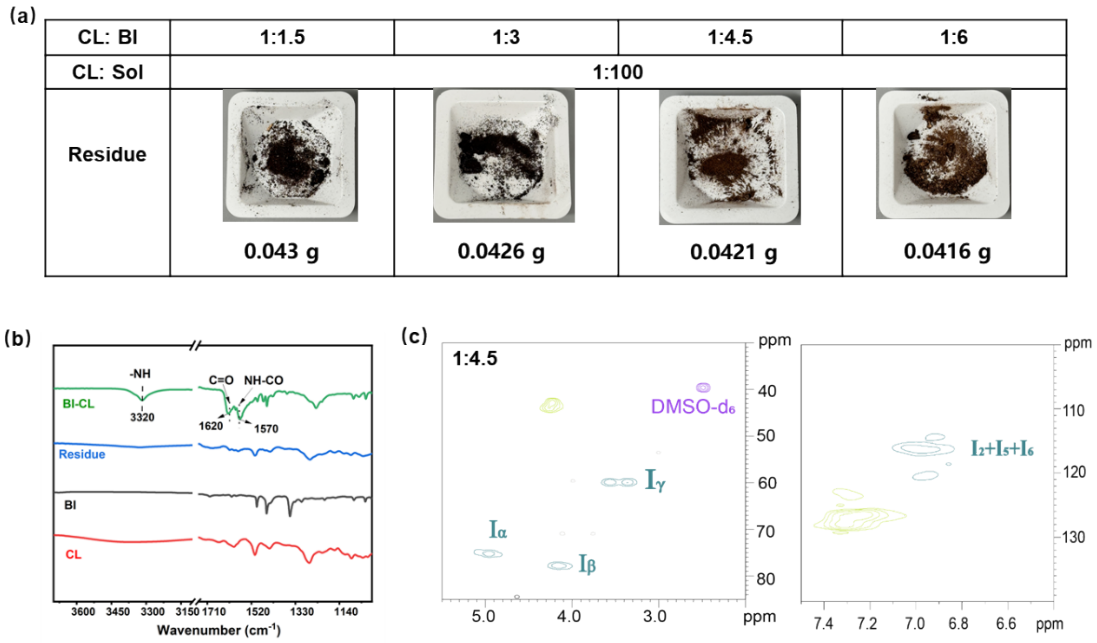

48

49 **Figure S8.** (a) The yield of residue under different conditions, (b) the FITR of CL, BI, residue, and
50 BI-CL (1:4.5,1:100), and (c) 2D-HSQC of residue (1:4.5,1:100)

51

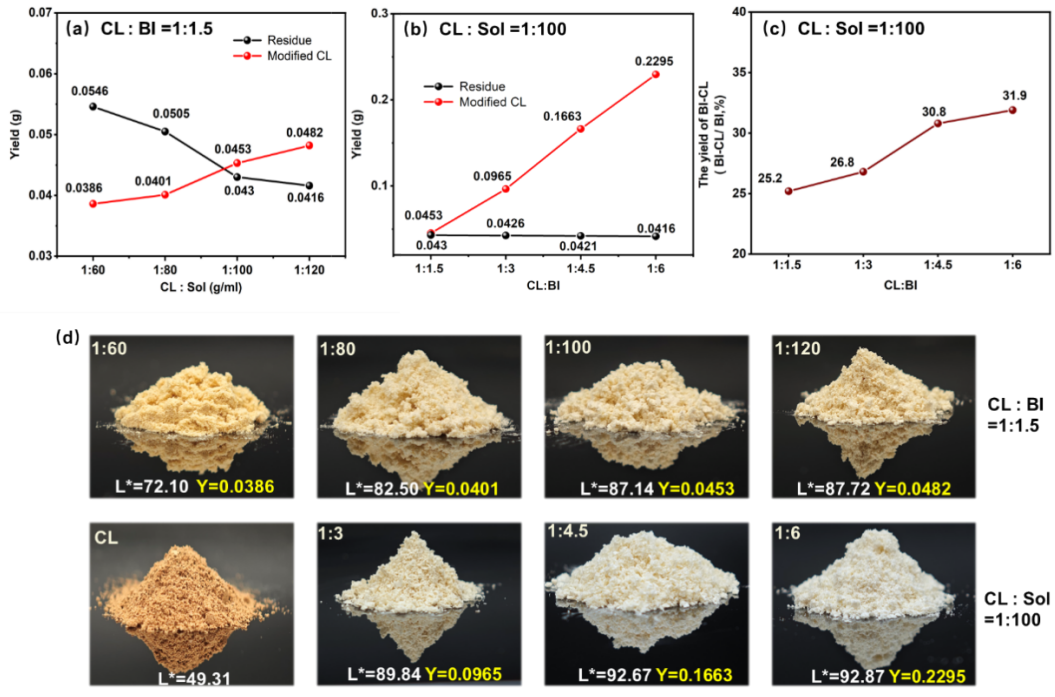

52

53 **Figure S9.** (a) The yield of products with different ratios of C-lignin (CL) to solvent at CL:
54 BI=1:1.5, (b) the yield of products under different CL: BI ratio at CL: Sol =1:100 (c) the yield of
55 BI-CL (BI-CL/BI, %), and (d) the lightness (L*) and yield (Y) of the samples.

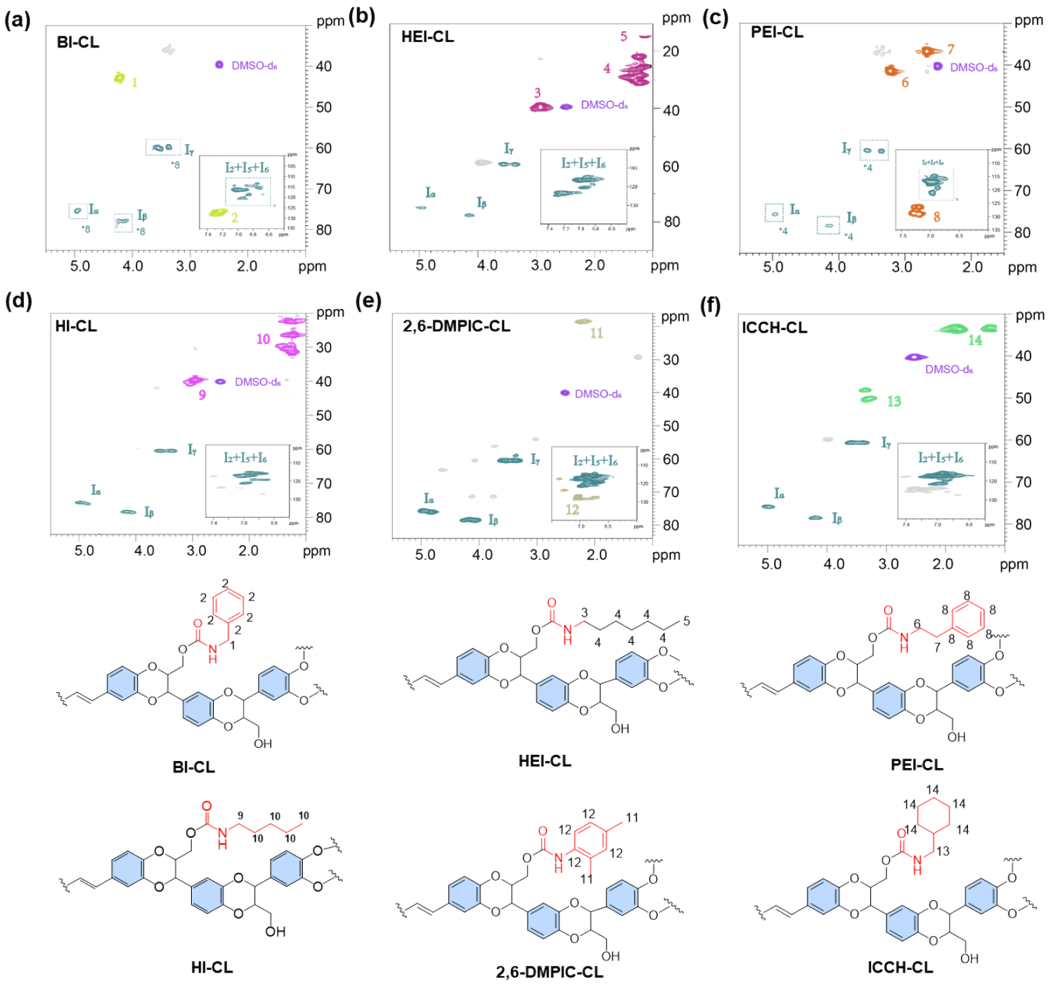

Figure S10. 2D HSQC NMR spectrum of CL modified by (a) BI, (b) HEI, (c) PEI, (d) HI, (e) 2,6-DMPIC, (f) ICCH

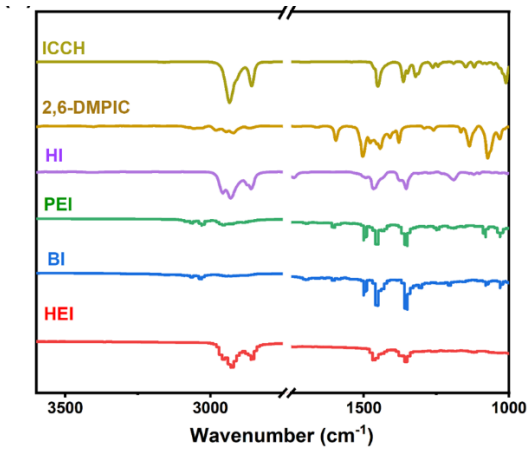

Figure S11. FTIR of (a) HEI, BI, PEI, HI, 2,6-DMPIC, and ICCH

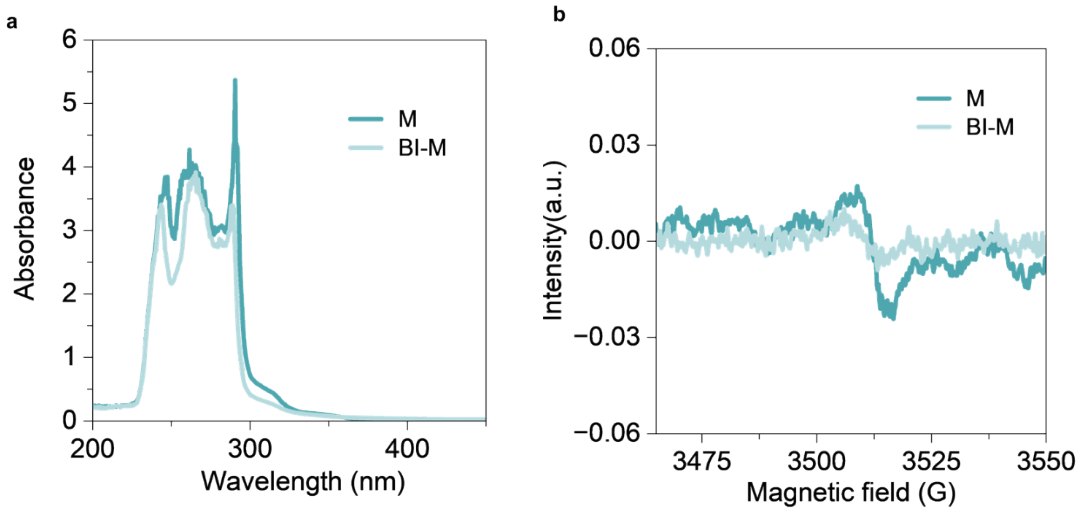

Figure S12. a) UV–vis and b) EPR spectra of M and BI-M recorded under identical conditions. BI-M exhibits a modest reduction in long-wavelength absorption and radical intensity relative to M.

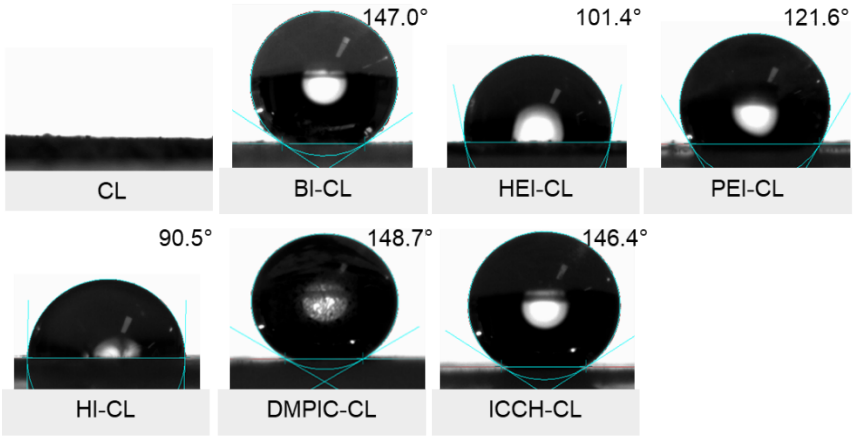

Figure S13. Water contact angel of CL, HEI-CL, BI-CL, PEI-CL, HI-CL, 2,6-DMPIC-CL, and ICCH-CL.

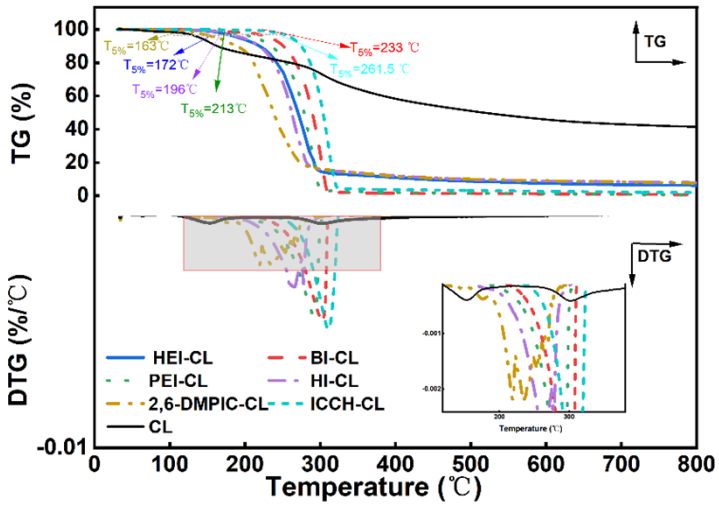

Figure S14. TG/DTG of CL, HEI-CL, BI-CL, PEI-CL, HI-CL, 2,6-DMPIC-CL, and ICCH-CL.

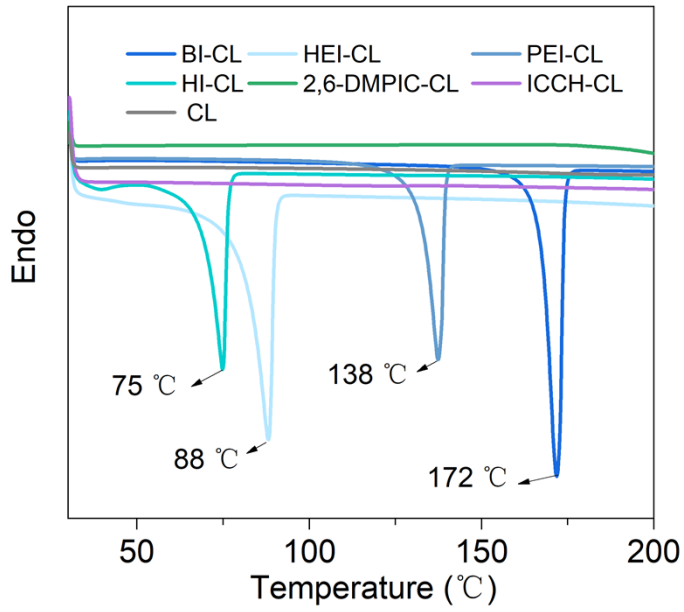

Figure S15. DSC of CL, HEI-CL, BI-CL, PEI-CL, HI-CL, 2,6-DMPIC-CL, and ICCH-CL

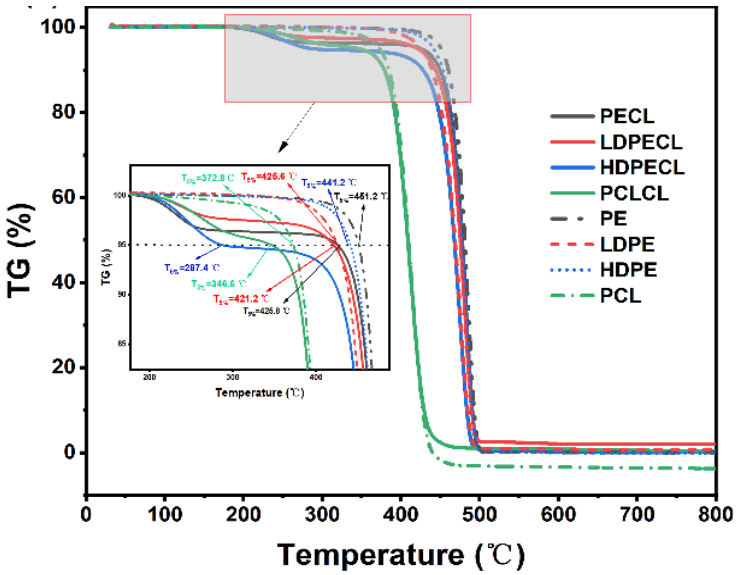

Figure S16. TG of corresponding films made by modified BI-CL mixing with different plastics and plastics alone.

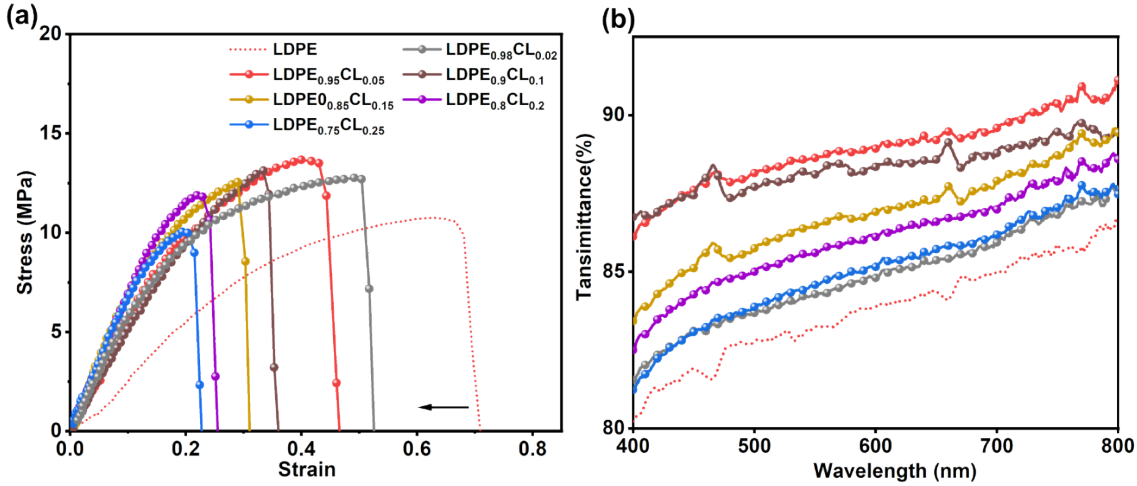

Figure S17. (a) The strain and stress curve of LDPE/BI-CL with different lignin content, and (b) the transmittance of LDPE/BI-CL with different lignin content in the visible light region (400-800 nm).

Table S1. NMR data for the signal assignments in C-lignin derivatives in DMSO-d_6.

Label	δ_C/δ_H (ppm)	Assignment
I_α	75.4/4.83	C_α-H_α in benzodioxane substructures (I)
I_β	77.9/4.06	C_β-H_β in benzodioxane substructures (I)
I_γ	59.9/3.34-3.55	Cγ-Hγ in benzodioxane substructures (I)
I_2, I_5, I_6	115.8/6.77, 116.5/6.95, 118.6/6.70, 120.4/6.95	C_2-H_2, C_5-H_5, C_6-H_6, in catechol units (I)
1	45.1/4.23	Benzyl group in γ-isocyanate-functionalized benzodioxane substructures
2	126.7-128.5/7.27-7.31	Benzyl group in γ-isocyanate-functionalized benzodioxane substructures
3	40.3/3.18	Heptyl group in γ-isocyanate-functionalized benzodioxane substructures
4	22.7-31.8/1.26-1.50	Heptyl group in γ-isocyanate-functionalized benzodioxane substructures
5	14.1/0.88	Heptyl group in γ-isocyanate-functionalized benzodioxane substructures
6	39.9/3.03	Phenethyl group in γ-isocyanate-functionalized benzodioxane substructures
7	35.0/2.74	Phenethyl group in γ-isocyanate-functionalized benzodioxane substructures
8	125.9-128.6/7.19-7.25	Phenethyl group in γ-isocyanate-functionalized benzodioxane substructures
9	40.3/3.18	Hexyl group in γ-isocyanate-functionalized benzodioxane substructures
10	14.1-29.6/0.88-1.50	Hexyl group in γ-isocyanate-functionalized benzodioxane substructures
11	17.6-21.6/2.16-2.24	2,6-Dimethylphenyl group in γ-isocyanate-functionalized benzodioxane substructures
12	126.2-143.4/6.95-7.15	2,6-Dimethylphenyl group in γ-isocyanate-functionalized benzodioxane substructures
13	43.8/2.88	Cyclohexyl group in γ-isocyanate-functionalized benzodioxane substructures
14	25.5-37.8/1.46-1.62;1.38-1.44	Cyclohexyl group in γ-isocyanate-functionalized benzodioxane substructures

Table S2. The yield of residue and modified CL by six isocyanates

Modified CL	Residue	Modified CL
BI-CL	0.0421	0.167
HEI-CL	0.0688	0.111
PEI-CL	0.0285	0.154
HI-CL	0.0327	0.163
2,6-DMPIC-CL	0.078	0.117
ICCH-CL	0.0241	0.158
CL	0.0421	0.167

Table S3. The hydroxyl group contents of CL, BI-CL under different CL: BI ratios (millimoles per gram)

CL: BI	Aliphatic-OH	-COOH	Catechol-OH			Total Catechol-OH
			a	b	c	
1:1.5	0.64	0.30	0.09	0.06	0.04	0.19
1:3	0.53	0.39	0.01	0.08	0.08	0.17
1:4.5	0.30	0.01	0.01	0.05	0.02	0.08
1:6	0.28	0.38	0.02	0.08	0.28	0.38
CL	8.36	0.26	-	3.09	2.70	5.79

Table S4. The hydroxyl group contents of CL, HEI-CL, BI-CL, PEI-CL, HI-CL, 2,6-DMPIC-CL, and ICCH-CL (millimoles per gram)

Modified CL	Aliphatic-OH	-COOH	Catechol-OH			Total Catechol-OH
			a	b	c	
HEI-CL	1.09	0.01	0.06	0.19	0.49	0.74
BI-CL	0.30	0.01	0.02	0.08	0.28	0.08
PEI-CL	0.48	-	0.04	0.02	0.40	0.46
HI-CL	0.53	0.10	0.33	0.28	0.09	0.70
2,6-DMPIC-CL	1.48	0.15	0.47	0.05	0.14	0.66
ICCH-CL	1.21	0.01	0.04	0.09	0.11	0.24
CL	8.36	0.26	-	3.09	2.70	5.79

Table S5. APC spectra of different CL samples

Sample	Product	M_w (Daltons)	M_n (Daltons)	PDI
CL	-	3164	2475	1.28
HEI-CL	Residue	3401	3392	1.20
	Product	2799	2463	1.14
BI-CL	Residue	4293	3991	1.18
	Product	1817	1756	1.03
PEI-CL	Residue	3818	3715	1.17
	Product	2202	2067	1.07
HI-CL	Residue	4036	4153	1.16
	Product	2547	2296	1.11
2,6-DMPIC-CL	Residue	3711	3651	1.21
	Product	2361	2157	1.09
ICCH-CL	Residue	3916	3617	1.27
	Product	2751	2255	1.22

Sample	L^*	a^*	b^*	ΔE
Standard	8.83	-1.53	1.32	-
CL	49.31	6.79	17.22	43.40
CL1.5BI	87.14	2.28	15.56	14.84
CL3BI	89.84	1.39	7.88	7.25
CL4.5BI	92.67	0.35	9.17	8.94
CL6BI	92.87	1.03	7.76	8.02
CLSol60	72.10	5.13	25.32	30.00
CLSol80	82.50	3.28	17.81	18.31
CLSol100	87.14	2.28	15.56	14.84

Table S6. The hydrophobicity of isocyanates

Solvent	XLogP3	iLab2.0	SILICOS-IT	MolSoft	ChemDraw	LogP
2,6-DMPIC	4.06	4.12	3.94	4.18	3.98	4.08
PEI	3.46	3.51	3.38	3.55	3.42	3.50
HEI	3.48	3.52	3.61	3.45	3.39	3.49
HI	3.01	3.03	3.11	2.98	2.95	3.02
BI	2.78	2.84	2.92	2.81	2.73	2.81
ICCH	2.71	2.78	2.85	2.69	2.66	2.74

CLSol120	87.72	1.92	14.36	13.53
BI-CL	92.67	0.35	9.17	8.94
HEI-CL	78.53	3.55	14.73	17.66
PEI-CL	89.24	0.75	12.41	11.33
HI-CL	75.49	4.43	29.38	31.64
2,6-DMPIC-CL	71.68	5.30	18.80	25.42
ICCH-CL	76.97	5.02	18.56	21.93

Table S7. L* a* b*(CIELAB) color space of different CL derivatives

Table S8. L* a* b*(CIELAB) color space of previous work

	Lignin type	Whitening Strategy	L*	ΔE	Ref.
1			88.6	1.27	
2	Kraft lignin	Isocyanate modification	89.72	1.82	[1]
3			88.59	1.46	
4			82.48	50.8	
5	Kraft lignin	Isocyanate modification	74.13	21.5	[2]
6			70.41	28.8	
7			77.9	29.2	
8	Kraft lignin	Isocyanate modification	78.1	27.4	[3]
9			76.6	28.2	
10	Biomass-derived lignin	Lignin-first strategy	71.53	26.5	[4]

11	Ethanol-extracted lignin	Ultrasound-assisted ethanol extraction	65.63	43.7	[5]
12	Alkali lignin	Nanoparticle formation	51.01	44.5	[6]
13	Kraft/Organosolv	Morphology control	49.03	29.4	[7]
14			71.6	35.5	
15	Various lignins	Structural analysis study	66.8	36.8	[8]
16			55.1	47.8	
17	Kraft lignin	Microsphere fabrication	61.68	36.8	[9]
18	Organosolv lignin	Cosolvent fractionation	37.69	63.81	[10]
19	DES lignin	Ternary DES extraction	62.96	33	[11]
20	Formic acid/phenol lignin	FA/phenol + ultrasound	80.2	29.3	[12]
21	Modified lignin	α-carbon methoxy substitution	73.0	25.2	[13]
22	Pine lignin	Phenolation + p-TsOH	72.3	16.4	[14]
23	Bamboo lignin	p-TsOH + THFA	86.1	19.2	[15]
24	Ultrafiltration lignin	Membrane fractionation	85.02	18.9	[16]
25	DES lignin	Controlled depolymerization	88.3	3.86	[17]
26	Catechyl lignin	Isocyanate modification	79.54	12.3	[18]

Table S9. Summary of trend-level correlations across multi-modal characterization.

Category	Parameter	Measurement	Trend	Nature of Evidence
Chemical conversion	Hydroxyl consumption	^{31}P NMR	↑	Direct
Radical signature	EPR intensity	EPR (DI)	↓	Direct
Electronic absorption	400–600 nm area	UV–vis	↓	Direct
Emissive states	PL intensity	PL	↓	Direct
Optical property	L^*	CIELAB color space	↑	Direct
Optical stability	Radical growth (in situ)	UV–EPR	↓	Direct

Category	Parameter	Measurement	Trend	Nature of Evidence
Interfacial modulation	Hydrophobicity	Contact angle	↑	Supporting

Table S10. The transmittance and haze of films produced by the previous work

	Transmittance (%)	Haze (%)	Ref.
1	92.24	13	[19]
2	78	22	[20]
3	80	32	[21]
4	43	30	[22]
5	49	35	[23]
6	68	28	[24]
7	62	30	[25]
8	70	13	[26]
9	85	64.4	[27]
10	72	69	[28]
11	85	93	[29]
12	75	70	[30]
13	78	62	[31]
14	59	97	[32]
15	44	65	[33]
16	87	50	Our work
17	83	65	Our work
18	80	80	Our work
19	78	90	Our work

Reference

[1] K. Shikinaka, Y. Otsuka, Functional "permanently whitened" lignin synthesized via solvent-controlled encapsulation, Green Chemistry 24(8) (2022) 3243-3249. https://doi.org/10.1039/D1GC04810D.

[2] S. Gao, X. Chen, G. Tian, et al., Preparation of light-colored bio-based particles by isocyanate-modified lignins and its application for tetracycline adsorption, International Journal of Biological Macromolecules 253 (2023) 127107. https://doi.org/https://doi.org/10.1016/j.ijbiomac.2023.127107.

[3] J. Zheng, L. Chen, X. Qiu, Y. Liu, Y. Qin, Structure investigation of light-colored lignin extracted by Lewis acid-based deep eutectic solvent from softwood, Bioresource Technology 385 (2023) 129458. https://doi.org/https://doi.org/10.1016/j.biortech.2023.129458.

[4] Z. Pan, Y. Li, Z. Zhang, et al., Fractionation of light-colored lignin via lignin-first strategy and enhancement of cellulose saccharification towards biomass valorization, Industrial Crops and Products 186 (2022) 115173. https://doi.org/https://doi.org/10.1016/j.indcrop.2022.115173.

[5] X. Su, Y. Fu, Z. Shao, et al., Light-colored lignin isolated from poplar by ultrasound-assisted ethanol extraction: Structural features and anti-ultraviolet and anti-oxidation activities, Industrial Crops and Products 176 (2022) 114359. https://doi.org/https://doi.org/10.1016/j.indcrop.2021.114359.

[6] H. Zhang, F. Chen, X. Liu, S. Fu, Micromorphology Influence on the Color Performance of Lignin and Its Application in Guiding the Preparation of Light-colored Lignin

232 Sunscreen, ACS Sustainable Chemistry & Engineering 6(9) (2018) 12532-12540.
233 https://doi.org/10.1021/acssuschemeng.8b03464.
234 [7] H. Zhang, S. Fu, Y. Chen, Basic understanding of the color distinction of lignin and
235 the proper selection of lignin in color-depended utilizations, International Journal of
236 Biological Macromolecules 147 (2020) 607-615.
237 https://doi.org/https://doi.org/10.1016/j.ijbiomac.2020.01.105.
238 [8] S.C. Lee, E. Yoo, S.H. Lee, K. Won, Preparation and Application of Light-Colored Lignin
239 Nanoparticles for Broad-Spectrum Sunscreens, Polymers 12(3) (2020) 699.
240 [9] H. Zhang, X. Liu, S. Fu, Y. Chen, Fabrication of Light-Colored Lignin Microspheres for
241 Developing Natural Sunscreens with Favorable UV Absorbability and Staining
242 Resistance, Industrial & Engineering Chemistry Research 58(31) (2019) 13858-13867.
243 https://doi.org/10.1021/acs.iecr.9b02086.
244 [10] Z. Li, L. Chen, X. Qiu, Fractionation of lignin using eco-friendly organic cosolvent
245 and preparation of light-colored lignin micro-nanoparticles for sustainable natural
246 sunscreens, Industrial Crops and Products 208 (2024) 117857.
247 https://doi.org/https://doi.org/10.1016/j.indcrop.2023.117857.
248 [11] C. Lu, J. Xu, J. Xie, et al., Preparation, characterization of light-colored lignin from
249 corn stover by new ternary deep eutectic solvent extraction, International Journal of
250 Biological Macromolecules 222 (2022) 2512-2522.
251 https://doi.org/https://doi.org/10.1016/j.ijbiomac.2022.10.035.
252 [12] Y. Wu, X. Chen, S. Ni, et al., Extracting light-colored lignin with high phenolic-OH
253 from poplar by ultrasonic-assisted formic acid/phenol treatment to prepare transparent

lignin/cellulose composite film, International Journal of Biological Macromolecules 309 (2025) 142840. https://doi.org/https://doi.org/10.1016/j.ijbiomac.2025.142840.

[13] S. Hua, S. Fu, B. Zhang, H. Liu, K. Xu, Methoxy substitution in the α-carbon of lignin side-chain inhibits its condensation for light-colored lignin extraction, International Journal of Biological Macromolecules 320 (2025) 145822. https://doi.org/https://doi.org/10.1016/j.ijbiomac.2025.145822.

[14] J. Zhang, Z. Tian, X.-X. Ji, F. Zhang, Light-colored lignin extraction by ultrafiltration membrane fractionation for lignin nanoparticles preparation as UV-blocking sunscreen, International Journal of Biological Macromolecules 231 (2023) 123244. https://doi.org/https://doi.org/10.1016/j.ijbiomac.2023.123244.

[15] H. Kong, X. Chen, S. Ni, et al., Targeted phenolation and rapid extraction of light-colored lignin from pine using nucleophilic reagent in combination with acid hydrotrope p-TsOH, Industrial Crops and Products 229 (2025) 120965. https://doi.org/https://doi.org/10.1016/j.indcrop.2025.120965.

[16] S. Wang, M.-F. Li, Efficient extraction of light-colored lignin from bamboo by p-toluenesulfonic acid assisted tetrahydrofurfuryl alcohol aqueous solution, International Journal of Biological Macromolecules 282 (2024) 136723. https://doi.org/https://doi.org/10.1016/j.ijbiomac.2024.136723.

[17] K. Shikinaka, A. Suzuki, Y. Otsuka, Substituent Effect on Physical Properties of Whitening Lignin, ChemistrySelect 9(26) (2024) e202400046. https://doi.org/https://doi.org/10.1002/slct.202400046.

[18] S. Su, Q. Shen, S. Wang, G. Song, Discovery, disassembly, depolymerization and derivatization of catechyl lignin in Chinese tallow seed coats, International Journal of Biological Macromolecules 239 (2023) 124256. https://doi.org/https://doi.org/10.1016/j.ijbiomac.2023.124256.

[19] X. Li, J. Li, X. Shen, et al., Transparent Cellulose/Lignin Composite Films with Adjustable Haze and UV-Blocking Performance for Light Management, ACS Sustainable Chemistry & Engineering 12(14) (2024) 5427-5435. https://doi.org/10.1021/acssuschemeng.3c07076.

[20] Q. Gu, T.L. Eberhardt, J. Shao, H. Pan, Preparation of an oxyalkylated lignin-g-polylactic acid copolymer to improve the compatibility of an organosolv lignin in blended poly(lactic acid) films, Journal of Applied Polymer Science 139(16) (2022) 52003. https://doi.org/https://doi.org/10.1002/app.52003.

[21] S.Y. Park, J.-Y. Kim, H.J. Youn, J.W. Choi, Utilization of lignin fractions in UV resistant lignin-PLA biocomposites via lignin-lactide grafting, International Journal of Biological Macromolecules 138 (2019) 1029-1034. https://doi.org/https://doi.org/10.1016/j.ijbiomac.2019.07.157.

[22] Q. Xing, D. Ruch, P. Dubois, L. Wu, W.-J. Wang, Biodegradable and High-Performance Poly(butylene adipate-co-terephthalate)–Lignin UV-Blocking Films, ACS Sustainable Chemistry & Engineering 5(11) (2017) 10342-10351. https://doi.org/10.1021/acssuschemeng.7b02370.

[23] Q. Xing, P. Buono, D. Ruch, et al., Biodegradable UV-Blocking Films through Core–Shell Lignin–Melanin Nanoparticles in Poly(butylene adipate-co-terephthalate), ACS

297 Sustainable Chemistry & Engineering 7(4) (2019) 4147-4157.
298 https://doi.org/10.1021/acssuschemeng.8b05755.
299 [24] X. Gu, J. Hou, S. Ai, Effect of silane modified nano-SiO2 on the mechanical properties
300 and compatibility of PBAT/lignin composite films, Journal of Applied Polymer Science
301 139(18) (2022) 52051. https://doi.org/https://doi.org/10.1002/app.52051.
302 [25] B. Lin, C. Li, F. Chen, C. Liu, Continuous Blown Film Preparation of High Starch
303 Content Composite Films with High Ultraviolet Aging Resistance and Excellent
304 Mechanical Properties, Polymers, 2021, p. 3813.
305 [26] X. Zhang, W. Liu, D. Yang, X. Qiu, Biomimetic Supertough and Strong Biodegradable
306 Polymeric Materials with Improved Thermal Properties and Excellent UV-Blocking
307 Performance, Adv. Funct. Mater. 29(4) (2019) 1806912.
308 https://doi.org/https://doi.org/10.1002/adfm.201806912.
309 [27] X. Wang, H. Guo, Z. Lu, et al., Lignin Nanoparticles: Promising Sustainable Building
310 Blocks of Photoluminescent and Haze Films for Improving Efficiency of Solar Cells, ACS
311 Applied Materials & Interfaces 13(28) (2021) 33536-33545.
312 https://doi.org/10.1021/acsami.1c08209.
313 [28] H. Ye, Y. He, H. Li, T. You, F. Xu, 3D-Printed Polylactic Acid/Lignin Films with Great
314 Mechanical Properties and Tunable Functionalities towards Superior UV-Shielding,
315 Haze, and Antioxidant Properties, Polymers 15(13) (2023) 2806.
316 [29] W. Zhang, X. Zhang, S. Ren, et al., Lignin containing cellulose nanofiber based
317 nanopapers with ultrahigh optical transmittance and haze, Cellulose 30(9) (2023) 5967-
318 5985. https://doi.org/10.1007/s10570-023-05244-2.

[30] T. Zheng, L. Yang, X.-F. Zhang, J. Yao, Conversion of corncob residue to sustainable lignin/cellulose film with efficient ultraviolet-blocking property, Industrial Crops and Products 196 (2023) 116517. https://doi.org/https://doi.org/10.1016/j.indcrop.2023.116517.

[31] Y. Jeon, K. Lee, Y. Seo, et al., Lignin-tailored lignocellulose nanofiber films for light management using a deep eutectic solvent, Chemical Engineering Journal 520 (2025) 165989. https://doi.org/https://doi.org/10.1016/j.cej.2025.165989.

[32] J. Li, X. Zhang, J. Zhang, et al., Direct and complete utilization of agricultural straw to fabricate all-biomass films with high-strength, high-haze and UV-shielding properties, Carbohydrate Polymers 223 (2019) 115057. https://doi.org/https://doi.org/10.1016/j.carbpol.2019.115057.

[33] R. Nizamov, J. Kaschuk, Y. Al Haj, et al., Optical assessment of lignin-containing nanocellulose films under extended sunlight exposure, Cellulose 32(9) (2025) 5321-5334. https://doi.org/10.1007/s10570-025-06380-7.